Crystallization behaviour and drug release from bacterial polyhydroxyalkanoates

Saghir Akhtar*, Colin W. Pouton and Lidia J. Notarianni
School of Pharmacy and Pharmacology, University of Bath, Bath, UK
(Received 10 October 1990; accepted 4 January 1991)

Crystalline polyhydroxyalkanoates (PHAs) such as poly-D(−)3-hydroxybutyrate (PHB) and its copolymers with poly-3-hydroxyvalerate (P(HB-HV)) are produced by a wide variety of bacteria and have uses in controlled drug delivery systems. The crystallization kinetics and morphology of P(HB-HV) polyesters both with and without the incorporation of a model drug, Methyl Red, have been investigated, as they are thought to influence drug release characteristics. The influence of copolymer composition and incorporation of Methyl Red on radial growth rates, G, of PHB and P(HB-HV) copolymer spherulites were investigated using polarized light video-microscopy. Growth curves could be obtained over a wide range of undercoolings for all the copolymers studied. At a given crystallization temperature, G decreased with increasing HV content and with increasing drug concentration in polymer spherulites. Spherulite morphology appeared to be a complex function of polymer molecular weight, copolymer composition, drug loading and crystallization temperature (T_c). Release of Methyl Red from melt-crystallized matrices of these PHAs was a function of T_c and copolymer composition. Drug release from isothermally crystallized copolymer films occurred progressively more rapidly with increasing HV content. This could be explained by the progressively poorer drug entrapment within copolymer matrices with increasing HV content. In PHB, Methyl Red was thought to be largely entrapped within spherulites (interlamellar regions) but for copolymers with increasing HV content, progressively greater amounts of drug were excluded at the spherulite surface and at interspherulitic boundaries.

(Keywords: poly-D(−)-3-hydroxybutyrate; poly-3-hydroxyvalerate; crystallization kinetics; crystalline morphology; drug distribution; drug delivery)

INTRODUCTION

Poly-D(−)-3-hydroxybutyrate (PHB) and its statistically random copolymers with poly-3-hydroxyvalerate (P(HB-HV)) are optically active, crystalline polyesters produced by a wide variety of microorganisms. PHB and P(HB-HV) copolymers are the most widely known of the polyhydroxyalkanoate (PHA) family of biodegradable biopolymers which are produced as energy reserve materials in such microorganisms as soil bacteria, estuarine microflora, blue green algae and microbially treated sewage[1–3]. PHAs are accumulated in discrete, membrane-bound granules within the cytoplasm of microbial cells. The polymers can be extracted from the cells in a relatively pure form using organic solvents such as chloroform or by membrane rupturing techniques such as mechanical, chemical and enzymatic disruption of cell walls[2]. The chemical structure of P(HB-HV) copolymers is given in *Figure 1*.

The exceptional purity, which has recently been confirmed by analysis with static secondary ion mass spectroscopy and X-ray photon spectroscopy[4], and chemical regularity of the homopolymer, PHB, make it an ideal model substance for fundamental studies of polymer crystallization, morphology and nucleation[5,6]. Indeed, the crystallization kinetics and morphology of the pure homopolymer[6] and as blends with polyethylene oxide[7] have been reported recently.

In addition, favourable biocompatibility and biodegradation properties of P(HB-HV) biopolymers have led to their investigation as matrices for controlled drug delivery[3,8–11]. Drug delivery devices employing thermoplastic PHB and P(HB-HV) copolymers are likely to be manufactured on a large scale using melt-processing technology. Although PHB is melt unstable with a narrow thermal processing window, copolymers with increasing HV content exhibit progressively larger processing windows and are thermally more stable[9]. PHB is reported to be relatively hard and brittle[12]. The mechanical properties of PHB can, however, be improved by copolymerization with HV and it has been suggested that the copolymers may be preferable for manufacture and implantation[3,12].

PHB and P(HB-HV) copolymers have been reported to undergo heterogeneous (surface) degradation[13] and as such offer the potential for producing drug delivery devices with predictable release kinetics of the active. Drug release from P(HB-HV) copolymers is thought to be dependent on HV content (as are other physico-mechanical properties[9,12]). This phenomenon cannot easily be explained in terms of the overall degree of

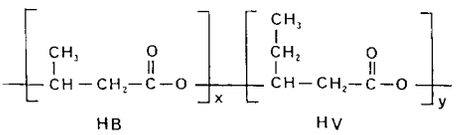

Figure 1 Chemical structure of P(HB-HV) copolymers

* Present address: Department of Pharmaceutical Sciences, University of Aston, Aston Triangle, Birmingham B4 7ET, UK

0032-3861/92/010117-10

crystallinity in these polymers, which has been reported to be independent of copolymer composition[14,15]. It is therefore thought that drug release behaviour (and other properties) of P(HB-HV) copolyesters may be better explained by differences in copolymer morphology. This paper describes the results of studies on the crystallization kinetics and morphology of melt-crystallized P(HB-HV) copolymers and examines how these factors influence the drug distribution and release profiles of a model drug, Methyl Red, when the drug is incorporated into polymer matrices.

MATERIALS AND METHODS

PHB homopolymers ($\bar{M}_w$ = 43 000, 380 000 and 770 000) and P(HB-HV) copolymers containing 7, 12 and 16 mol% HV (PHV6, PHV12 and PHV16 respectively) were produced by the bacterial fermentation of a glucose-utilizing mutant of *Alcaligenes eutrophus* and were purchased from Marlborough Biopolymers Ltd, UK.

Methyl Red (2-[[4-(diamino)phenyl]azo]-benzoic acid) was purchased from BDH Chemicals, Poole, UK.

Purification of polymers

Although the 'as supplied' polymers were of a medical grade, they were further purified as a routine procedure. Purification was achieved by refluxing in chloroform (2% w/v), filtering the polymer solutions (Whatman no. 52 filter paper) and recrystallizing with excess methanol. The recrystallized polymers were washed with water and methanol and dried in a vacuum oven at 45°C for 12 h.

Characterization of polymers

Determination of copolymer composition. The HV contents of P(HB-HV) copolymers were determined by ^{1}H n.m.r. according to the method described by Bloembergen *et al.*[14].

^{1}H n.m.r. spectra of 1% w/v solutions of P(HB-HV) copolymers in deuterated chloroform were recorded using a Jeol GX-270MHZ spectrometer in the pulse Fourier transform mode. A pulse repetition of 5.5 s was employed with a 3 kHz spectral width, 32 000 data points and 100 accumulations. The HV content (expressed as mol%) was calculated from the relative magnitudes of the integrated areas of the methyl resonances in the side groups of HB and HV monomeric repeating units.

Determination of polymer molecular weight. The molecular weight distributions of the biopolymers were determined by gel permeation chromatography (g.p.c.) according to the method described by Majid[16,17]. Briefly, 20 μl polymer samples (1% w/v) in chloroform were injected into a mixed-PL gel (5 μm) column, 0.3 cm × 30 cm (Polymer Labs, UK), previously calibrated with polystyrene (PS) standards (Polymer Labs, UK). A mobile phase of HPLC grade chloroform at 25°C was used and eluent detection was achieved using an i.r. spectrophotometer (Perkin Elmer 782) set at 1760 cm^{-1} to detect the carbonyl (C=O) resonance characteristic of P(HB-HV) biopolymers. PS detection was based on the C–H stretch occurring at 2730 cm^{-1}. Data were stored and analysed using a BBC Master microprocessor interfaced to the i.r. detector. Mark–Houwink constants used were $K = 1.065 \times 10^{-2}$ ml g^{-1}, $\alpha = 0.728$ for PS, and $K = 1.510 \times 10^{-2}$ ml g^{-1}, $\alpha = 0.756$ for PHB, as quoted by Majid[16,17].

The molecular characteristics of the polymers used are summarized in *Table 1*.

Solvent casting of polymer films

Polymer films (30–50 μm) were cast from chloroform solution (4% w/v) onto dry, degreased glass plates using a thin layer chromatography applicator with an adjustable clearance. In the case of drug-loaded films, Methyl Red (a model drug) was also incorporated into the polymer–chloroform solution prior to film casting.

Crystallization kinetics and morphology

All polymer samples were used as solution-cast films except for PHV16 which was used in purified powder form. Samples (2–3 mg) of PHB and P(HB-HV) copolymers were heated to melt between two thin glass slides at 195°C for 30–60 s on a Monotherm hot plate (Rodwell Scientific Instruments Ltd). Polymer samples were then rapidly transferred to a Mettler FP82 hot stage linked to a Mettler FP80 central processor programmed for isothermal heating at a chosen crystallization temperature, T_c. The hot stage was connected to a polarizing optical microscope (Vickers) and radial growth of spherulites was recorded onto videotape using a Hitachi colour video camera with a V102 vertical enhancer (Hitachi Denshi Ltd, Japan) and a Panasonic AG6200 VHS video cassette recorder. Spherulite radius, R, was measured directly from a calibrated flat monitor screen as a function of time, t, and radial growth rate was derived from the slope of the linear plot of R *versus* t. The mean of at least three growth rate measurements for each temperature was recorded.

For the determination of equilibrium melting temperatures, data on observed melting temperatures, T_m, were

Table 1 Molecular characteristics of PHB and P(HB-HV) copolymers

Polymer	Symbol	Batch no.	HV content (mol%)		$\bar{M}_w$ ($\times 10^3$)	$\bar{M}_n$ ($\times 10^3$)	$\bar{M}_w/\bar{M}_n$
			Nominal (ICI)	^{1}H n.m.r.			
PHB	PHB43K	BX T82	0	0	43	29	1.48
PHB	PHB800K	BX GV9	0	0	765	506	1.51
PHB	PHB380K	BX T41	0	0	384	226	1.70
P(HB-HV)	PHV6	BX PV6	6.60	7.47	410	267	1.53
P(HB-HV)	PHV12	BX PV12	12.60	11.99	1293	908	1.42
P(HB-HV)	PHV16	BX PV16	15.90	16.21	41	27	1.51

obtained as follows. As soon as the polymer spherulites had filled all the available space, that is impingement occurred, the temperature was raised at a programmed heating rate of 10 K min^{-1} and the melting point of the sample, crystallized isothermally at T_c, was optically determined by observing the disappearance of the birefringence pattern.

Drug release studies

Release studies with isothermally crystallized films (30–50 μm) containing Methyl Red were carried out in vials containing 25 ml phosphate buffer (pH 7.4) at 37°C. Vials were shaken in a waterbath at a frequency of 180 oscillations min^{-1}. In order to maintain conditions close to sink, variable amounts of release medium were removed periodically and replaced with equivalent amounts of fresh buffer. Release of Methyl Red was determined spectrophotometrically at 430 nm.

RESULTS AND DISCUSSION

Equilibrium melting temperature of PHB and P(HB-HV) copolymers

The determination of equilibrium melting temperatures (T_m^0) of PHB and P(HB-HV) copolymers from optical microscopy data are shown in *Figure 2* and summarized in *Table 2*. For all the copolymer compositions used in this study, plots of observed melting temperature (T_m) against crystallization temperature (T_c) exhibited linear relationships. The Hoffman–Weeks equation[18]:

$$T_m = T_c/\gamma + (1 + 1/\gamma)T_m^0 \quad (1)$$

was found to fit the experimental data well and hence allowed reproducible values of T_m^0 to be determined from extrapolations of the T_m *versus* T_c plots. The value of 197°C for the equilibrium melting temperature of PHB ($\bar{M}_w$ = 380000) obtained in this study is similar to that of 196°C reported by Greco and Martuscelli[19] and agrees well with those of 195°C and 194°C reported by Barham *et al.*[6] and by Avella and Martuscelli[7] respectively. The minor discrepancies may be explained by differences in polymer molecular weight. Indeed, we find that PHB of low polydispersities (below 2) in the range $\bar{M}_w$ = 43000–770000 exhibit values of T_m^0 in the range 193–197°C (*Table 2*).

The T_m^0 values of P(HB-HV) copolymers progressively decreased with increasing HV content from a value of 197°C for the homopolymer to 167°C for the copolymer containing 16 mol% HV (PHV16), (see *Figure 2b* and *Table 2*).

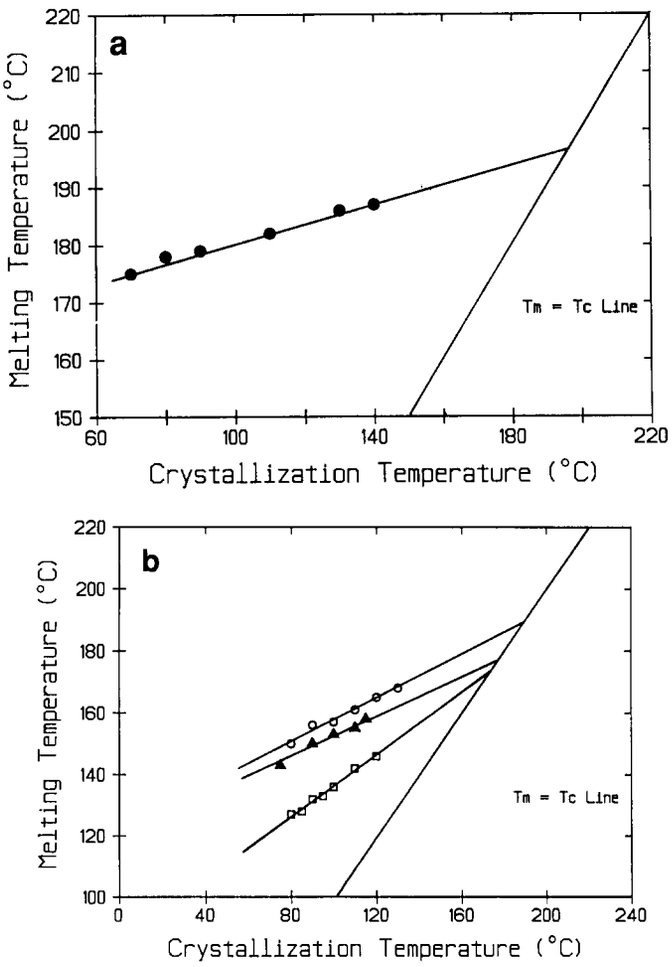

Figure 2 Equilibrium melting point determinations from T_m *versus* T_c plots for (a) PHB380K and (b) P(HB-HV) copolymers containing 7 mol% HV (PHV6); ▲, 12 mol% HV (PHV12); □, 16 mol% HV (PHV16)

Table 2 Summary of equilibrium melting temperatures for PHB and P(HB-HV) copolymers

Polymer	T_m^0 (°C)
PHB43K	193
PHB380K	197
PHB800K	197
PHV6	186
PHV12	173
PHV16	167

Crystallization kinetics of pure P(HB-HV) copolymers

At any given crystallization temperature, T_c, growth rates of PHB and P(HB-HV) copolymers were linear for all copolymer compositions studied. This suggested that a consistent concentration of polymer molecules was present at the growth front for PHB and its copolymers. The radial growth rates of spherulites of P(HB-HV) copolymers were influenced by copolymer composition. Under isothermal conditions, copolymers with increasing HV content crystallized from the melt with progressively slower growth rates. This is shown in *Figure 3a* where radial growth rates of spherulites are plotted as a function of crystallization temperature for a range of copolymer compositions (0–16 mol% HV). A plot of maximal growth rate, G_{max}, of isothermally crystallized polymer spherulites against copolymer composition shows that the relationship was not linear (see *Figure 3b*). The inclusion of only 7 mol% HV (PHV6) into the homopolymer reduced G_{max} to 32%, whereas inclusion of 12 mol% (PHV12) and 16 mol% HV (PHV16) reduced G_{max} to 11% and 5%, respectively, when compared to the value of G_{max} obtained for the homopolymer, PHB380K. In addition, G_{max} was also achieved at progressively lower crystallization temperatures with increasing HV content. The peak in the growth curve for PHB occurred at 90°C whereas the growth curve for PHV16 reached a peak at 70°C. This reflects (within the bounds of experimental error) the depression

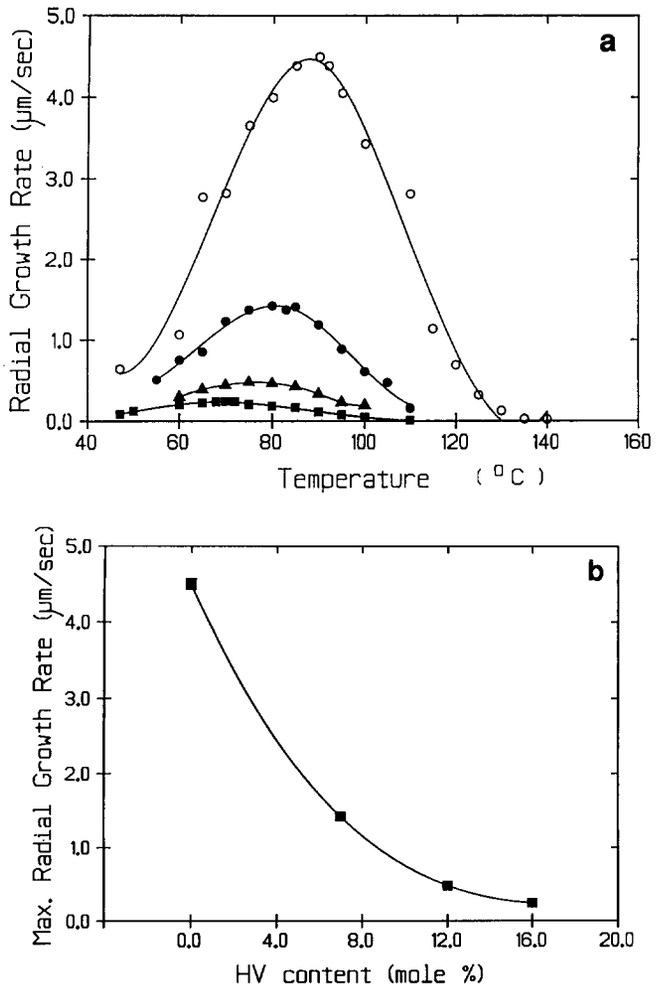

Figure 3 (a) Radial growth rates of PHB and P(HB-HV) copolymer spherulites *versus* crystallization temperature: ○, PHB380K; ●, PHV12; ▲, PHV12; ■, PHV16. (b) Maximal growth rates (G_{max}) of PHB and P(HB-HV) copolymer spherulites as a function of copolymer composition (HV content)

in equilibrium melting point of the copolymer (see *Table 2*) and emphasizes the fact that G_{max} is governed by the undercooling (as postulated by Hoffman *et al.*[20]). Indeed G_{max}, or the peak in the growth profile, of all the copolymers studied occurred at a similar undercooling (ΔT) to that observed for the homopolymer, PHB380K (ΔT of around 100°C).

The progressively slower radial growth rates for P(HB-HV) copolymer spherulites with increasing HV content was thought to be due to the retarded incorporation of the HV components into the common crystal lattice. This was thought to be largely due to the slower transport of chain segments containing HV components to the crystal growth front, arising from the larger molar mass of this comonomer. However, the extent to which HV components are incorporated into the PHB crystal lattice remains unclear. Although Marchessault and co-workers[14,15] suggest that P(HB-HV) copolymers are isodimorphic and therefore the HV components would be expected to be equally distributed between the amorphous and crystalline domains, recent evidence has questioned this hypothesis[21]. If the degree of crystallinity of the copolymers is similar, then equal distribution of HV components between crystal and amorphous domains cannot account for the decreasing density of copolymer samples with increasing HV content[21]. There may be some exclusion of HV from crystals.

Thermodynamic parameters from data on crystallization kinetics

The equation of Hoffman *et al.*[20] is thought to govern the spherulite growth rate *versus* temperature profiles. The linear growth rate (G) of polymer spherulites is given as:

$$G = G_0 \exp[-U^*/R(T - T_\infty)] \exp[-K_g(1/T\Delta T_f)] \quad (2)$$

where G_0 is a constant, U^* is an activation energy for transport of molecules to the growth front, R is the gas constant, T is the crystallization temperature, T_∞ is the temperature below which molecules become immobile and ΔT is the supercooling. In addition:

$$f = 2T/(T_m^0 + T) \quad (3)$$

and

$$K_g = Kb_0\sigma\sigma_e T_m^0/k\Delta H_F \quad (4)$$

where T_m^0 is the equilibrium melting temperature (melting temperature of infinitely thick, defect-free crystal), k is Boltzmann's constant, b_0 is the monomolecular layer thickness, ΔH_F is the heat of fusion, $\sigma\sigma_e$ is the product of the lateral and end surface free energies and K may have the value of 2 or 4 depending on the growth mechanism.

Hoffman *et al.*[20] originally proposed two different growth regimes in polymer crystals, depending on the relative rates of formation and spreading of new secondary nuclei at the growth front. Regime I is thought to occur at low supercoolings when the rate of spreading is so large compared to the rate of nucleation that a nucleus, once formed, spreads right across the growth front. Regime II occurs at higher or intermediate supercoolings when several secondary nuclei form and spread across the growth front together, the separation between them decreasing as the supercooling increases. More recently, Hoffman[22] has proposed a third regime of growth in polymer crystals: regime III is thought to occur at sufficiently high supercoolings when the separation between secondary nuclei is of the order of a molecular width and no more spreading takes place. The three regimes may be distinguished by the value of the constant K in the equation for K_g (equation (4)); in regimes I and III, $K = 4$ and in regime II, $K = 2$.

The data represented in the growth curves for P(HB-HV) polymers crystallized at high temperatures were used in an attempt to fit Hoffman's equation (2). In order to model this equation, values of T_m^0, U^* and T_∞ need to be estimated. T_m^0 values were deduced from T_m *versus* T_c plots and have been summarized in *Table 2*. Estimates of K_g, and hence an insight into the molecular mechanism of growth for PHB and P(HB-HV) copolymers, were made by obtaining best linear fits for the growth data when plotted in the form: $\log G + U^*R(T - T_\infty)$ against $1/T\Delta T_f$. Hoffman *et al.*[20] found that for a fairly large number of polymers, values of U^* in the vicinity of 1000–1400 cal mol^{-1} and T_∞ values about 30°C below T_g give excellent fits. Values of T_∞ of about 20–50°C below T_g and values of U^* in the range 0.9–1.20 kJ mol^{-1} gave good fits for P(HB-HV) polymers and the results are summarized in *Table 3*.

Table 3 Summary of best fit values for various parameters in equation (2)

Polymer	U^* (kJ mol^{-1})	T_∞ (K)	T_m^0 (K)	$K_g \times 10^5$ (K^2)	Regressional analysis, r^2
PHB380K	1.20	230	470	−4.83	0.993
PHV6	1.00	250	460	−2.24	0.980
PHV12	1.00	260	446	−1.30	0.957
PHV16	0.90	265	440	−2.75	0.996

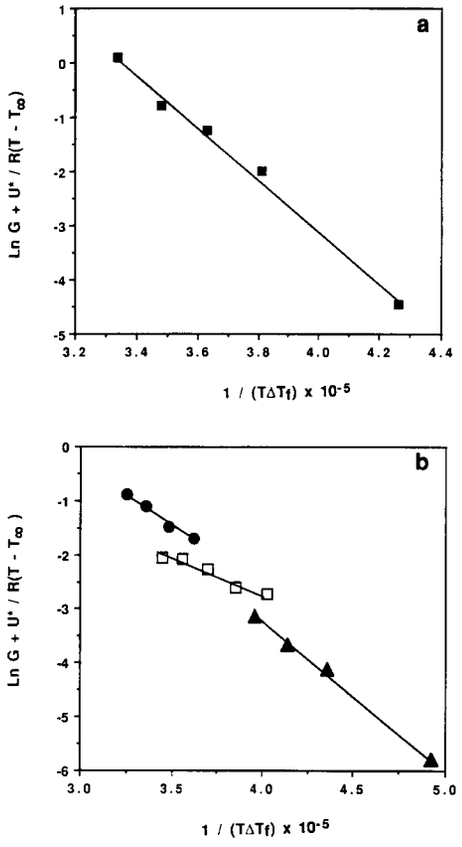

Figure 4 Best fits of crystallization data according to equation (2) for (a) PHB380K and (b) P(HB-HV) copolymers: ●, PHV6; □, PHV12; ▲, PHV16

The best-fit plots derived from the parameters in *Table 3* are plotted according to the Hoffman equation in *Figures 4a* and *b*. The slope or K_g values derived for PHB (from *Figure 4a*) and P(HB-HV) copolymers (from *Figure 4b*) from the fitted growth data at high crystallization temperatures is also given in *Table 3*. Barham *et al.*[6] found that PHB crystallizes according to regime III when crystallized at the undercoolings used in this study. This means that the K_g value obtained for PHB (see *Table 3*) corresponds to $K = 4$ in equation (4).

In the case of P(HB-HV) copolymers, PHV6 and PHV16 exhibited K_g values that were approximately half of that obtained for PHB380K. It must be concluded that these copolymers crystallize according to regime II ($K = 2$ in equation (4)) at the undercoolings studied. However, the K_g value of -1.3×10^5 K^2 for PHV12 does not adequately fit any of the regimes proposed by Hoffman *et al.*[20]. It is possible that the crystallization temperatures chosen for the fit of PHV12 fall at the intersection of two regimes resulting in an anomalous K_g value. Further studies are in progress to ascertain this fact and to locate regime intersections for a wide range of copolymers. It should be noted that regime I has not yet been observed for PHB[23]. This fact may lend support to the proposal of Point and Dosiere[24] who have concluded that regime I is hypothetical and does not occur in practice. Furthermore, the latter authors have severely criticized the use of ln G *versus* $1/T\Delta T$ plots to establish regime I and thereby have seriously questioned the validity of Hoffman's theory[20].

P(HB-HV) copolymer morphology from polarized light optical photomicrographs

For a given polymer, the internal fine structure and size of polymer spherulites was found to be dependent on crystallization temperature, T_c. *Figure 5* shows spherulites of PHB380K crystallized isothermally at three different temperatures. Banded spherulites for PHB were observed at some crystallization temperatures. Band spacing, when it occurs, has been reported[6] to increase with increasing T_c. Banded spherulites were also observed for P(HB-HV) copolymers.

Figure 6 shows optical photomicrographs (from polarized light microscopy) of PHB and P(HB-HV) copolymer spherulites isothermally crystallized at 90°C. Banding is clearly visible for PHV6 (*Figure 6d*) but is less obvious for the higher HV content copolymers at this crystallization temperature. The morphologies for the three different molecular weights of the homopolymer and the copolymers are clearly different from each other. Examination of the internal fine structure suggested that spherulitic morphology was a complex function of polymer molecular weight, crystallization temperature and copolymer composition. The way in which morphological differences in copolymer spherulites influence drug release profiles will be discussed below.

The effect of drug incorporation in P(HB-HV) polymers on spherulitic growth rates

Methyl Red (2-[[4-(diamino)phenyl]azo]-benzoic acid) is chloroform-soluble and was chosen as a model crystalline drug because its physicochemical characteristics resemble those of moderately lipophilic drugs. It also has a melting point[25] similar to that of the homopolymer PHB, at around 181–182°C. In addition, its red colour is easy to detect in release studies by a simple spectrophotometric assay. *Figure 7* shows that pure Methyl Red, in the absence of polymer, also crystallized from the melt as spherulites. In the presence of PHB (and P(HB-HV) copolymers), Methyl Red (at low concentrations below 2% w/w) did not crystallize as separate spherulites, suggesting that the drug remained amorphous during crystallization. At higher concentrations, some exclusion of Methyl Red was observed at the

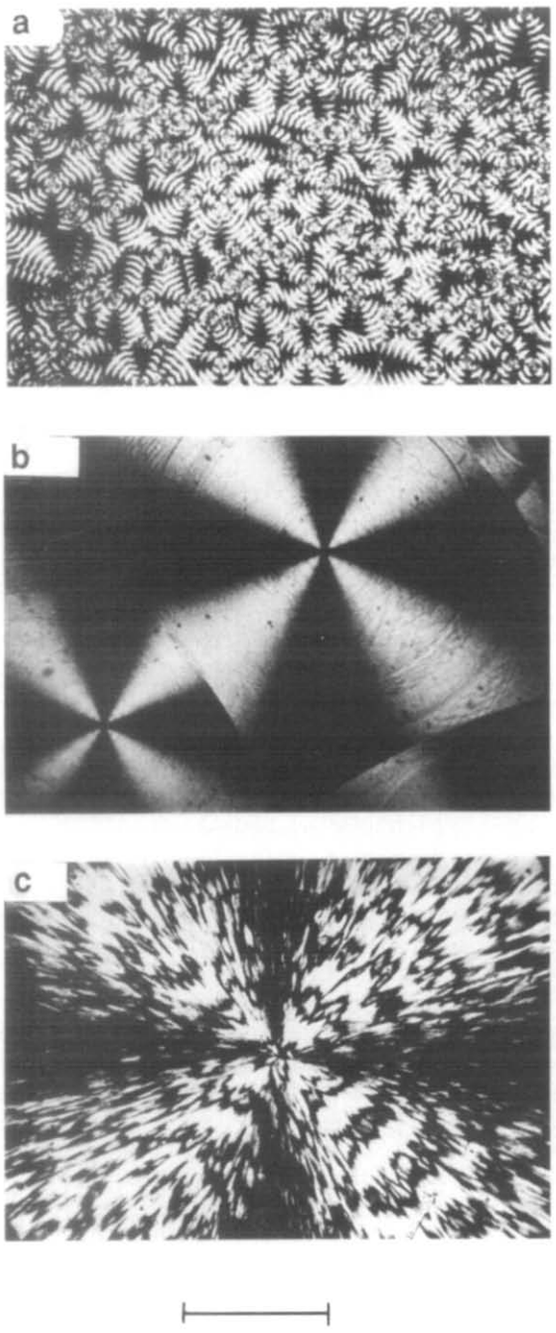

Figure 5 Morphology of PHB380K spherulites isothermally crystallized at (a) 60°C; (b) 90°C; (c) 110°C. Scale bar = 500 μm

higher crystallization temperatures where overall crystallization rates were very slow. No evidence of spherulite texture for the excluded drug was obtained from optical micrographs. In the main part, Methyl Red was thought to be entrapped within spherulite boundaries and within the interlamellar fibrils (see below). A similar conclusion has been derived[7] for blends of PHB and poly(ethylene oxide) (PEO). Although PEO is crystalline, it fails to crystallize in the presence of PHB and is thought to remain amorphous and possibly trapped within the interlamellar regions of PHB spherulites[7].

Figure 8 shows the radial growth rate *versus* temperature curves for PHB380K loaded with 2 and 8% w/w of Methyl Red as a model drug. The G_{max} was substantially reduced on increasing drug concentration. Loadings of only 2% w/w Methyl Red reduced G_{max} to 80% of that for pure polymer and at 8% w/w loading the G_{max} was only 59% of that for the pure homopolymer. An 8% loading of Methyl Red was sufficient not only to reduce the growth rate of PHB but also to cause a marginal shift in G_{max} to a lower crystallization temperature. Again, this was related to the depression in the T_m^0 of PHB380K containing 8% Methyl Red and therefore was a function of the undercooling. For PHB380K containing 8% Methyl Red, a T_m^0 of 189°C was obtained (determined as described above). Therefore the undercooling at which G_{max} occurred for PHB380K and PHB380K containing 8% Methyl Red was equivalent.

The effects of drug incorporation on the rate of polymer crystallization may be explained according to the theory of Keith and Padden[26,27]. This phenomenological theory proposed that molecular species which crystallize slowly, or cannot crystallize, will be regarded as impurities and will be rejected at the growth fronts of crystals. The rejected species (drug or impurities) then accumulate to give enhanced local concentrations, above average values in the melt, to magnitudes controlled by local diffusion fields. The reduced growth rate is observed because the accumulated drug or impurities at the growth interfaces depress the equilibrium (liquidus) temperature of the melt and therefore the under- or supercooling at the isothermal interface. Keith and Padden[26,27] showed that when the rejected species are sufficiently mobile, deviations from the linear growth rate were observed, often giving rise to parabolic growth behaviour. This was not observed for the concentrations of Methyl Red used in this study and growth rates remained linear for all the undercoolings investigated. This implied that the concentration of Methyl Red at the tips of radial fibres (chain folded lamellae) remained constant throughout growth. It has been suggested by Keith and Padden[26,27] that a steady state of this type can be maintained even in the presence of large concentrations of impurity (drug) up to extremely large spherulite sizes.

Drug release from melt-crystallized Methyl Red–polymer matrices

In an attempt to assess the effect of polymer morphology on drug release, PHB and P(HB-HV) films containing Methyl Red were isothermally crystallized at fixed temperatures to yield known morphologies and the rate of drug release was determined in each case.

Figure 9a shows the release of Methyl Red (8% w/w) from PHB380K films crystallized at either 60°C or 110°C to highlight the effect of crystallization temperature on release rate. The amount of drug released is clearly different for the two morphologies over the initial phase of release but converges to a similar value in the second phase of release. Films crystallized at 110°C exhibited a greater 'burst effect' (i.e. the rapid initial release of drug) than films prepared at 60°C. This suggests that the different crystalline morphologies obtained must entrap the same loading of drug to varying extents. The use of a coloured marker drug was clearly an advantage in discerning between polymer and drug under a light microscope. Examination of optical photomicrographs for drug-loaded polymer spherulites crystallized at 60 and 110°C showed that different distributions of drug existed within polymer films (*Figure 10*). It can be seen that greater amounts of Methyl Red (visible as dark

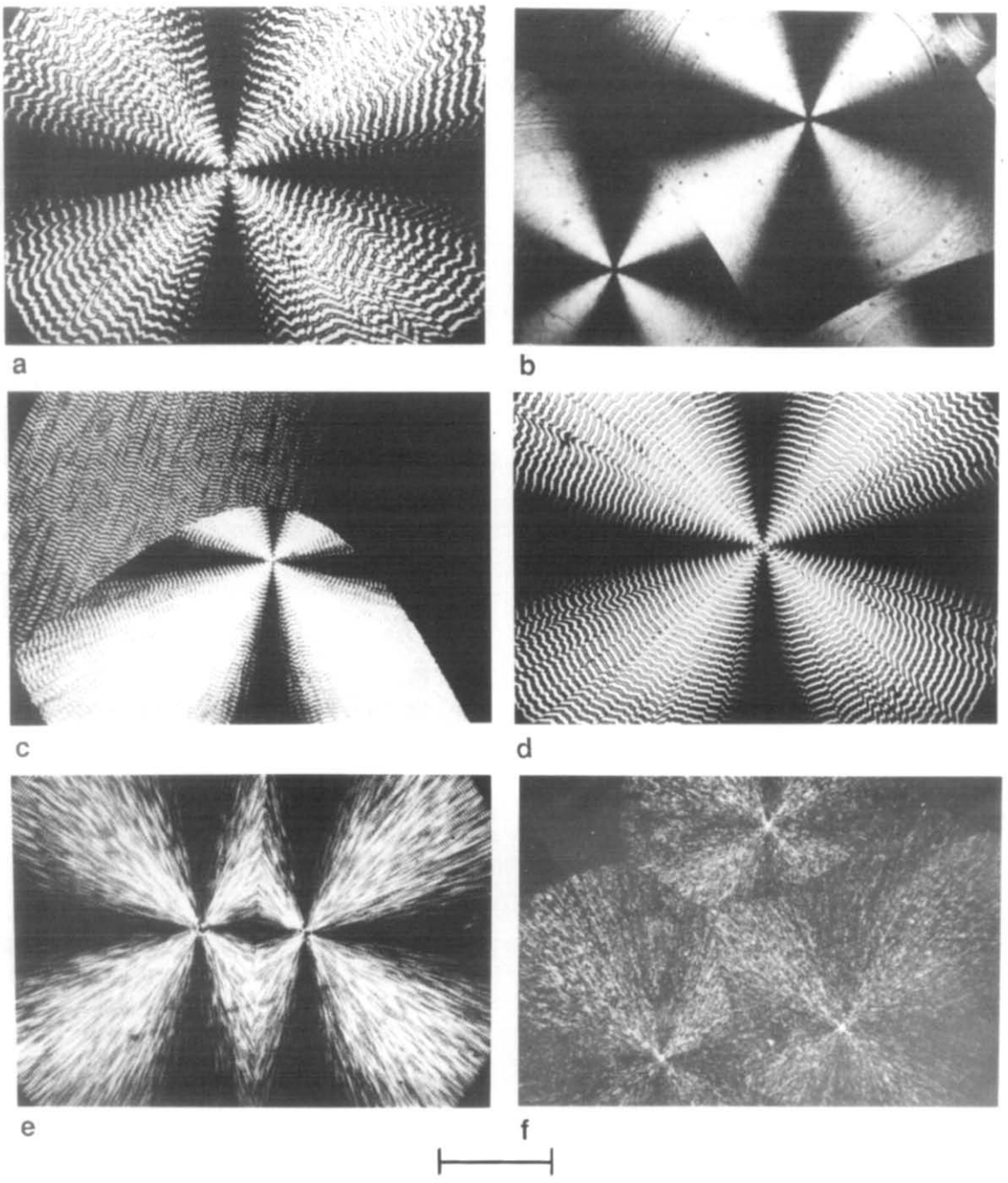

Figure 6 Morphology of PHB and P(HB-HV) copolymer spherulites isothermally crystallized at 90°C. (a) PHB43K; (b) PHB380K; (c) PHB800K; (d) PHV6; (e) PHV12; (f) PHV16. Scale bar = 500 μm

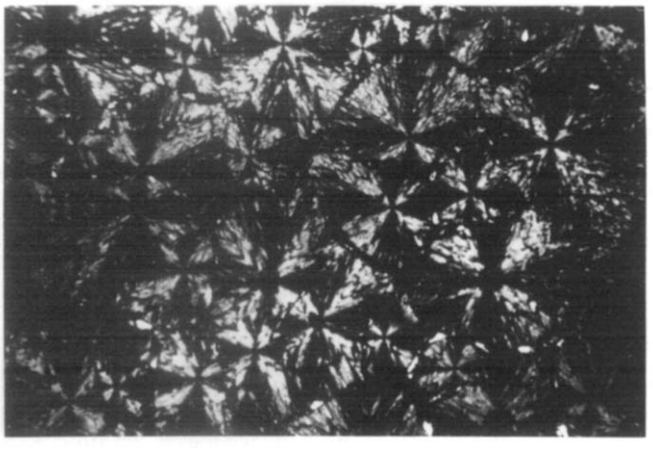

Figure 7 Spherulites of Methyl Red isothermally crystallized at 90°C

patches) were present at the surface of film matrices crystallized at 110°C (*Figure 10c*) compared to 60°C (*Figure 10a*) which led to the greater burst effect observed in the release profiles of the 110°C morphology. As a comparison, *Figure 10b* shows the morphology of PHB films also containing 8% w/w Methyl Red but crystallized at 90°C. These films, not used in drug release studies, appeared to have surface quantities of drug which were judged (by eye) to be intermediate to those seen for 60°C and 110°C morphologies. It should be noted that although G of PHB spherulites crystallized at 60°C was slightly slower, the overall rate of crystallization (a consequence of the greater nucleation rate of PHB spherulites at 60°C) was faster than for spherulites crystallized at 110°C. It was with the more rapid rates of overall crystallization that the drug became well

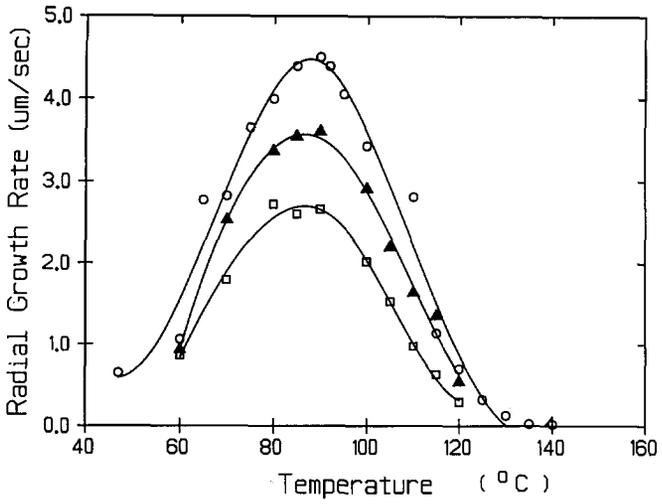

Figure 8 Plot of radial growth rates against crystallization temperature for PHB380K (○) and PHB380K spherulites containing different concentrations of Methyl Red: ▲, 2%; □, 8%

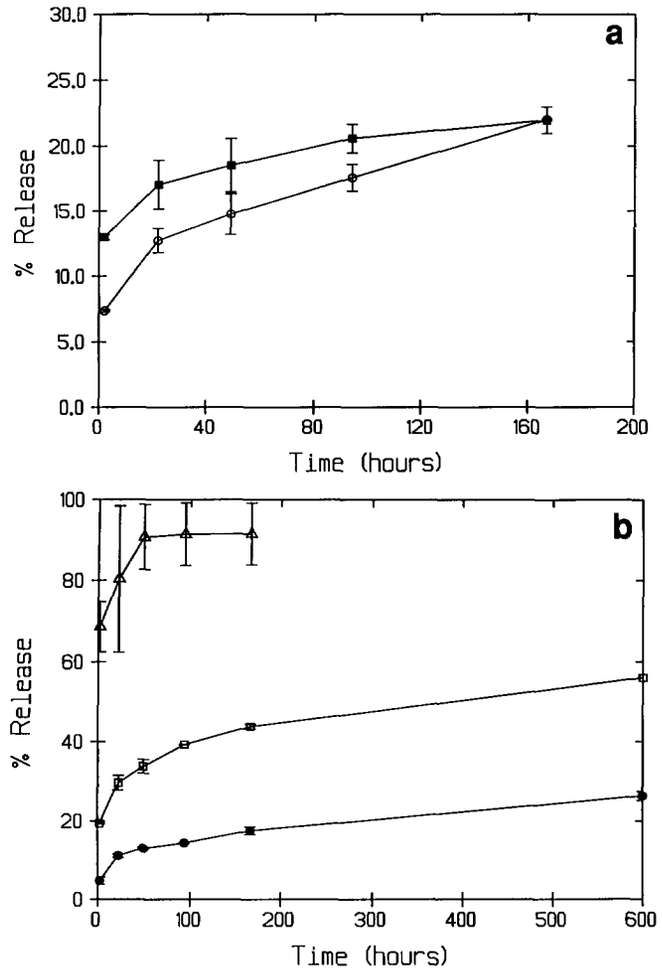

Figure 9 Drug release profiles: (a) Methyl Red-loaded PHB380K films isothermally crystallized at 60°C (○) and 110°C (■); (b) PHB380K (●) and P(HB-HV) copolymer films (□, PHV6; △, PHV12) isothermally crystallized at 90°C

trapped within spherulites. Hence in the case of the 60°C morphology, radial diffusion of rejected drug molecules was outstripped by the more rapid growth of chain folded lamellae so that drug was trapped in interlamellar channels. In the case of the 110°C morphology, the slower overall growth of chain folded lamellae allowed greater amounts of drug to be rejected from the growth front.

Figure 9b shows drug release from PHB and P(HB-HV) copolymer films containing 4% w/w Methyl Red isothermally crystallized at 90°C. With increasing HV content, the copolymer morphologies obtained at this temperature released drug at progressively faster rates than the homopolymer. After 100 h of release, PHV12 had released effectively all of the loaded drug whereas only about 40% was released from PHV6 and only about 15% from the homopolymer. This was explained by the fact that progressively slower rates of crystallization with increasing HV content produced crystalline morphologies in which drug was less well

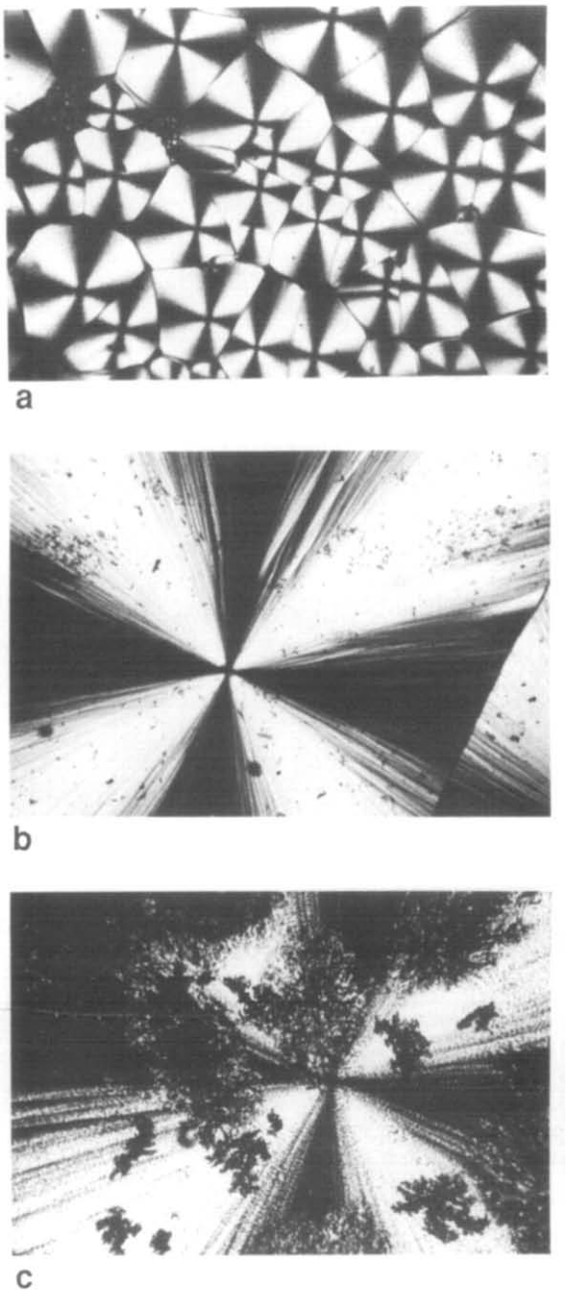

Figure 10 Spherulitic morphology of PHB380K films containing 8% w/w Methyl Red crystallized at (a) 60°C; (b) 90°C; (c) 110°C. Scale bar = 500 μm

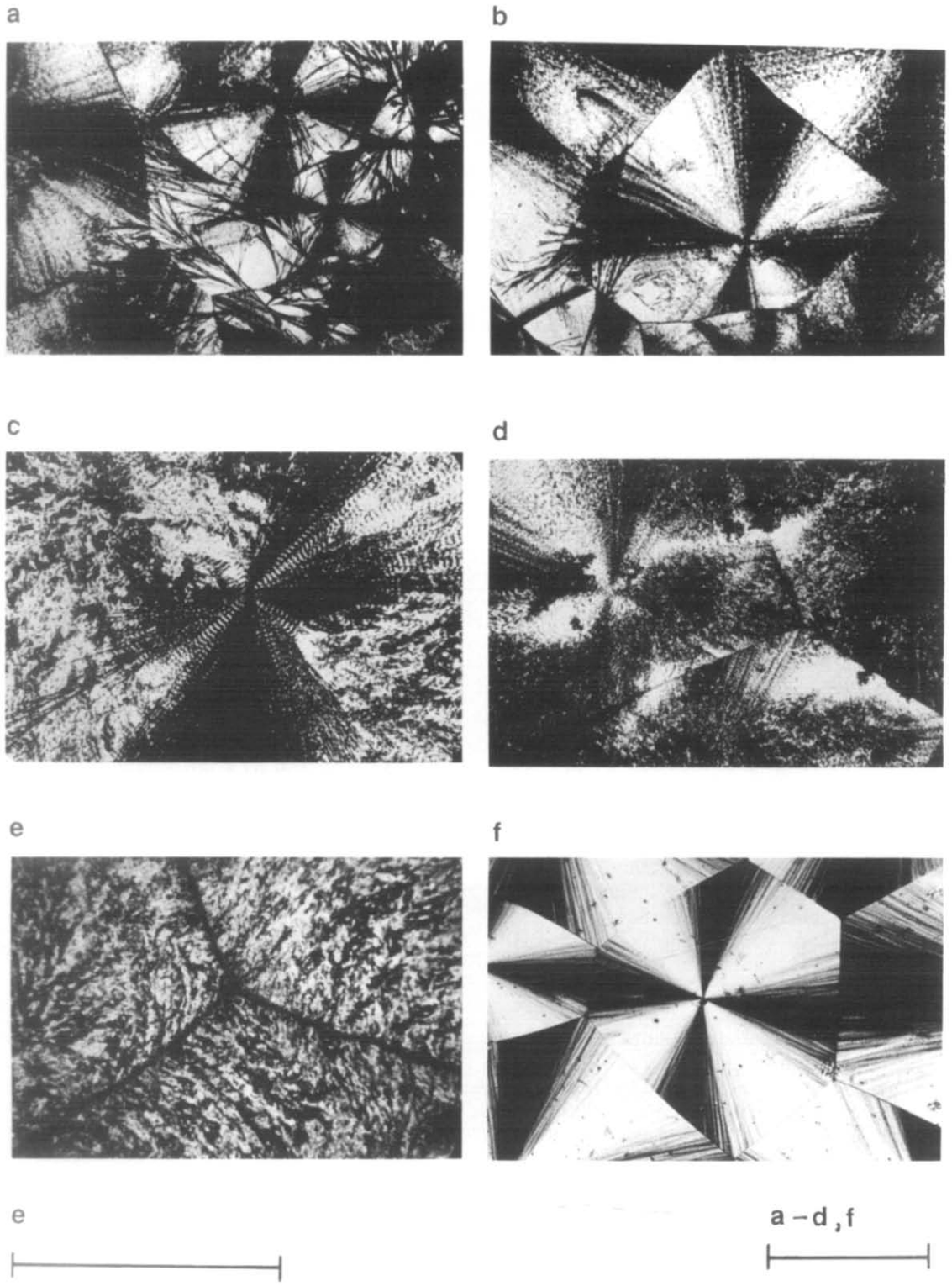

Figure 11 Spherulitic morphology of polymer films containing 4% w/w Methyl Red. (a), (b) PHV6; (c)–(e) PHV12; (f) PHB380K. Scale bars = 500 μm

trapped than in the homopolymer and in which progressively greater amounts of drug were excluded to the surface. This was confirmed by the optical micrographs of drug-loaded films shown in *Figure 11*. Compared with the homopolymer (*Figure 11f*), where little drug was expressed at the surface of spherulites, progressively greater amounts of drug (dark patches) were visible at the surface of PHV6 (*Figures 11a* and *b*) and PHV12 (*Figures 11c–e*) respectively. At greater magnification (*Figure 11e*) it could be seen in PHV12 that drug appeared to be present largely at the surface and at interspherulite boundaries (intersection of three spherulites is shown) which led to the majority of drug being released over a short period of time (see *Figure 9b*). This initial phase of release was thought to occur primarily by dissolution and diffusion removing drug present at (or close to) the surface of film matrices. The second phase of release, in which drug was released more

slowly, was thought to involve removal of drug entrapped within polymer spherulites (i.e. within interlamellar regions). This more tightly bound drug was thought to be released by the matrix-type mechanism proposed by Siegel *et al.*[28] and which we previously observed for P(HB-HV) copolymer matrices prepared by solvent casting[9,10].

P(HB-HV) copolymer degradation, which requires a period of 2 to 3 years for completion for a film of this thickness[3,13], was not thought to control release of Methyl Red over the time periods used in this study. However, polymer degradation is more likely to be a factor in controlling drug release from PHB matrices where only a small burst effect (for example see *Figure 9b*) was observed and where the relatively slower release of Methyl Red suggested that the drug was largely well trapped within intraspherulitic regions (possibly between the chain folded lamellae). Further studies are in progress to establish the intraspherulitic distribution of Methyl Red and certain other therapeutic drugs, such as peptide hormones. The ability to achieve a homogeneous distribution of drug within polymer matrices, such that drug release is controlled only by the slow degradation of the polymer, is a major technical barrier which needs to be overcome before P(HB-HV) systems realize their full potential in drug delivery.

CONCLUSIONS

The crystallization kinetics of PHB and P(HB-HV) copolymers have been investigated with and without the incorporation of a model drug, Methyl Red. At any given T_c, radial growth rates of polymer spherulites were reduced by increasing either drug loading or HV content.

The crystalline morphology of P(HB-HV) biopolymers was thought to be a complex function of polymer molecular weight, drug loading, crystallization temperature and copolymer composition. According to Hoffman's latest theory of crystallization[20,22] PHB crystallizes according to regime III at the crystallization temperatures studied (110–135°C). The PHV6 and PHV16 copolymers were thought to crystallize according to regime II at the respective undercoolings investigated. However, the crystallization data for PHV12 did not adequately fit any of the regimes proposed by Hoffman[22].

The entrapment and release of Methyl Red from melt-crystallized polymer matrices was a function of polymer crystallization kinetics and morphology. Release profiles of PHB films isothermally crystallized at 110°C exhibited a greater burst effect when compared to those crystallized at 60°C. This was explained by greater amounts of drug being excluded from spherulites during crystallization of films at 110°C. The progressively slower crystallization of copolymers with increasing HV content resulted in spherulitic morphologies with decreasing abilities to trap Methyl Red. Drug release from melt-crystallized copolymer films was therefore more rapid than from PHB and was a function of the HV content.

The above results indicate that by careful selection of copolymer composition and of processing temperatures during the isothermal crystallization of drug-loaded P(HB-HV) biopolymers, it is possible to produce drug delivery devices with tailored release kinetics.

ACKNOWLEDGEMENTS

The authors thank Drs P. J. Barham, S. Organ and P. A. Barker (H.H. Wills Physics Laboratory, University of Bristol, UK) for useful discussions on crystallization kinetics. The SERC are thanked for a CASE award to Dr S. Akhtar. The generous financial assistance from Cyanamid of Great Britain Limited, Gosport, UK is also acknowledged.

REFERENCES

1 Dawes, E. A. and Senior, P. J. *Adv. Microbial Phys.* 1973, **10**, 203
2 Lafferty, R. M., Korsatko, B. and Korsatko, W. in 'Biotechnology' (Eds H. J. Rehm and G. Reed), Vol. 6b 'Special Microbial Processes' (Ed. H. J. Rehm), VCH Verlagsgesellschaft, Weinheim, 1988, p. 135
3 Akhtar, S. and Pouton, C. W. *Drug News Perspect.* 1989, **2**, 89
4 Davies, M. C., Khan, M. A., Short, R. D., Akhtar, S., Pouton, C. and Watts, J. F. *Biomaterials* 1990, **11**, 228
5 Barham, P. J. *J. Mater. Sci.* 1984, **19**, 3826
6 Barham, P. J., Keller, A., Otun, E. L. and Holmes, P. A. *J. Mater. Sci.* 1984, **19**, 2781
7 Avella, M. and Martuscelli, E. *Polymer* 1988, **29**, 1731
8 Gould, P. L., Holland, S. J. and Tighe, B. J. *Int. J. Pharm.* 1987, **38**, 231
9 Akhtar, S. *PhD Thesis* University of Bath, UK, 1990
10 Akhtar, S., Pouton, C. W., Notarianni, L. J. and Gould, P. L. *J. Pharm. Pharmacol.* 1989, **41**, 5P
11 Brophy, M. R. and Deasy, P. B. *Int. J. Pharm.* 1986, **29**, 223
12 Akhtar, S., Pouton, C. W., Notarianni, L. J. and Gould, P. L. *J. Pharm. Pharmacol.* 1987, **39**, 43P
13 Pouton, C. W., Majid, M. I. A. and Notarianni, L. J. *Proc. Int. Symp. Control. Rel. Bioact. Mater.* 1988, **15**, 181
14 Bloembergen, S., Holden, D., Hamer, G. K., Bluhm, T. L. and Marchessault, R. H. *Macromolecules* 1986, **19**, 2865
15 Bluhm, T. L., Hamer, G. K., Marchessault, R. H., Fyfe, C. A. and Veregin, R. P. *Macromolecules* 1986, **19**, 2871
16 Majid, M. I. A. *PhD Thesis* University of Bath, UK, 1988
17 Majid, M. I. A., Pouton, C. W. and Notarianni, L. J. *J. Pharm. Pharmacol.* 1987, **39**, 34P
18 Hoffman, J. D. and Weeks, J. J. *J. Res. Natl Bur. Stand., A* 1962, **66**, 13
19 Greco, P. and Martuscelli, E. *Polymer* 1989, **30**, 1475
20 Hoffman, J. D., Davies, G. T. and Lauritzen, J. I. in 'Treatise on Solid State Chemistry', Vol. 3 (Ed. N. B. Hanney), Plenum Press, New York, 1976, p. 497
21 Barker, P. A., Mason, F. and Barham, P. J. *J. Mater. Sci.* 1990, **25**, 1952
22 Hoffman, J. D. *Polymer* 1983, **24**, 3
23 Barham, P. J. and Keller, A. *J. Appl. Polym. Sci., Polym. Phys. Edn* 1986, **24**, 69
24 Point, J. J. and Dosiere, M. *Polymer* 1989, **30**, 2292
25 Windholz, M. (Ed.) 'The Merck Index: An Encyclopedia of Chemicals, Drugs and Biologicals', 10th Edn, Merck and Co., Inc., Rahway, 1983
26 Keith, H. D. and Padden, F. J. *J. Appl. Phys.* 1964, **35**, 1270
27 Keith, H. D. and Padden, F. J. *J. Appl. Phys.* 1964, **35**, 1286
28 Siegel, R. A., Kost, J. and Langer, R. *J. Controlled Release* 1989, **8**, 223